Spectral representation for u- and t-channel exchange processes in a partial-wave decomposition

M. F. M. Lutz,[1] E. E. Kolomeitsev,[2] and C. L. Korpa[3]

[1]GSI Helmholtzzentrum für Schwerionenforschung GmbH, Planckstraße 1, 64291 Darmstadt, Germany
[2]Matej Bel University, Faculty of Natural Sciences, Tajovskeho 40, SK-97401 Banska Bystrica, Slovakia
[3]Department of Theoretical Physics, University of Pécs, Ifjúság útja 6, 7624 Pécs, Hungary

(Received 8 June 2015; published 15 July 2015)

We study the analytic structure of partial-wave amplitudes derived from u- and t-channel exchange processes. The latter plays a crucial role in dispersion-theory approaches to coupled-channel systems that model final state interactions in QCD. A general spectral representation is established that is valid in the presence of anomalous thresholds, decaying particles or overlapping left-hand and right-hand cut structures as it occurs frequently in hadron physics. The results are illustrated at hand of ten specific processes.

DOI: 10.1103/PhysRevD.92.016003 PACS numbers: 11.55.Bq, 11.55.Fv, 11.80.-m

I. INTRODUCTION

It is still an open challenge to derive final state interactions from QCD based on effective field theory approaches at energies where the strong interaction forms resonances. From the phenomenology of the last decades, it is known that coupled-channel unitarity together with the microcausality condition play a decisive role in the enterprise to unravel the underlying physics of this nonperturbative domain of QCD (see e.g. [1–14]).

While final state interactions close to an elastic threshold can be treated quite reliably in perturbation theory based on a suitable chiral Lagrangian this is not so for energies where the resonance spectrum is observed. A convenient framework to study final state interactions is based on the concept of a generalized potential. A partial-wave scattering amplitude $T_{ab}(s)$ with a channel index a and b for the final and the initial state, respectively, is decomposed into contributions from left- and right-hand cuts where all left-hand cut contributions reside in the generalized potential $U_{ab}(s)$. For an approximated generalized potential the right-hand cuts are induced by means of the nonlinear integral equation

$$T_{ab}(s) = U_{ab}(s) + \sum_{c,d} \int \frac{dw^2}{\pi} \frac{s-\mu_M^2}{w^2-\mu_M^2} \times \frac{T_{ac}^\dagger(w^2)\rho_{cd}(w^2)T_{db}(w^2)}{w^2-s-i\epsilon}, \quad (1)$$

where $\rho_{cd}(w^2)$ is a channel dependent phase-space function. By construction any solution of (1) does satisfy the coupled-channel s-channel unitarity condition. While the general framework is known from the 1960s [15–22], only recently has this framework been successfully integrated into an effective field theory approach based on the chiral Lagrangian. The main additional and novel idea is to approximate the generalized potential systematically by means of a conformal expansion that is reliable not only near the threshold but also in the resonance region. The key observation is that in (1) the generalized potential is needed only in the region where the partial-wave amplitude has its right-hand cuts. In this region a conformal expansion is reliable and systematic results can be expected. Since the expansion point for the conformal map can be dialed to lie within the convergence domain of strict chiral perturbation theory, the expansion coefficients may be computed from the chiral Lagrangian. First applications of this novel approach can be found in [10–14,23].

The conformal expansion of the generalized potential requires the detailed knowledge of the spectral representation of the generalized potential, the main target of the present work. The results of the following study are indispensable for the analytic extrapolation of the generalized potential into the resonance region. The analytic continuation of a function requires a thorough understanding of its branch points and lines [24]. The latter lead to its spectral representation. While for reactions involving stable particles it is straightforward to unravel the spectral representation of the generalized potential [25,26], this is not so for reactions involving, for instance, the nonet of vector mesons with $J^P = 1^-$ or the baryon decuplet states with $J^P = \frac{3}{2}^+$. The latter play a crucial role in the hadrogenesis conjecture that expects the low-lying resonance spectrum of QCD light with up, down and strange quarks only to be generated by final state interactions of the lowest SU(3) flavor multiplets with $J^P = 0^-, 1^-$ and $J^P = \frac{1}{2}^+, \frac{3}{2}^+$ [6–9,27–33]. The coupled-channel interaction of such degrees of freedom leads to a plethora of subtle phenomena, which need to be treated carefully. The left- and right-hand cuts may overlap and the generalized potential may be singular at threshold kinematics. The latter leads to an anomalous threshold behavior of the partial-wave scattering amplitudes. This may occur at a threshold but also at a

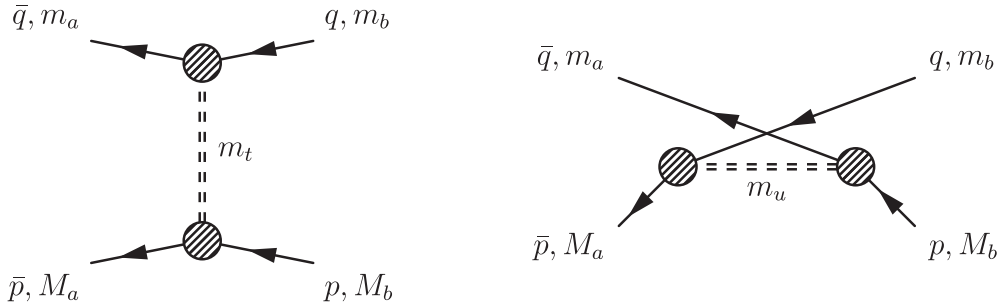

FIG. 1. Generic t- and u-channel exchange processes.

pseudothreshold. In this case, the nonlinear integral equation (1) has to be adapted properly.

The work is organized as follows. In Secs. II and III the framework for a dispersion-integral representation of partial-wave amplitudes is set up, and general results are derived. Detailed illustrations are offered with specific t-channel and u-channel diagrams in Sec. IV. We conclude with a short summary in Sec. V.

II. PARTIAL-WAVE PROJECTION OF INVARIANT SCATTERING AMPLITUDES

A general scattering amplitude $T(\bar{k},k;w)$ will have a decomposition into a set of invariant amplitudes $F_n(s,t,u)$ and associated tensors $L_n(\bar{k},k;w)$ that carry possible Dirac and Lorentz structure of the scattering amplitude. The latter is required for reactions of particles with nonvanishing spin. We write

$$T(\bar{k},k,w)=\sum_n F_n(s,t,u)L_n(\bar{k},k;w),$$
$$s=(p+q)^2,\qquad t=(p-q)^2,\qquad u=(p-\bar{q})^2, \quad (2)$$

where we insist on invariant amplitudes, $F_n(s,t,u)$, that are free of kinematical constraints [34–36]. Owing to energy and momentum conservation the scattering amplitude $T(\bar{k},k;w)$ depends on three 4-vectors $\bar{k}_\mu, k_\mu$ and w_μ only with

$$k=\frac{1}{2}(p-q),\qquad \bar{k}=\frac{1}{2}(\bar{p}-\bar{q}),\qquad w=p+q=\bar{p}+\bar{q}, \quad (3)$$

where p,q and $\bar{p},\bar{q}$ are the 4-momenta of the in and outgoing particles, respectively. A complete set of Dirac and Lorentz tensors $L_n(\bar{k},k;w)$ depends on the reaction considered. In the literature, such a decomposition has been worked out explicitly for various reactions [35,37–41].

The partial-wave scattering amplitudes are given by appropriate projection integrals,

$$T^{(JP)}(s)=\sum_n\int_{-1}^{+1}dx\lambda_n^{(JP)}(s,x)F_n(s,t[s,x],u[s,x]), \quad (4)$$

where $\lambda_n^{(JP)}(s,x)$ are functions of kinematic origin. They are derived in the literature for any given angular momentum J and parity P (see e.g. [37–43]). In (4) we consider $F_n(s,t,u)$ as functions of s and the cosine of the scattering angle $x=\cos\theta$. The main target of this work is the derivation of a spectral representation for such partial-wave amplitudes.

According to the hypothesis of Mandelstam [16], the amplitudes $F_n(s,t,u)$ satisfy dispersion integral representations characterized by a set of spectral weight functions,

$$\begin{aligned}F_n(s,t,u)&=\int_0^\infty\frac{d\bar{s}}{\pi}\frac{\rho_s^{(n)}(\bar{s})}{s-\bar{s}}+\int_0^\infty\frac{d\bar{t}}{\pi}\frac{\rho_t^{(n)}(\bar{t})}{t-\bar{t}}+\int_0^\infty\frac{d\bar{u}}{\pi}\frac{\rho_u^{(n)}(\bar{u})}{u-\bar{u}}\\&+\int_0^\infty\frac{d\bar{s}}{\pi}\int_0^\infty\frac{d\bar{t}}{\pi}\frac{\rho_{st}^{(n)}(\bar{s},\bar{t})}{(s-\bar{s})(t-\bar{t})}\\&+\int_0^\infty\frac{d\bar{t}}{\pi}\int_0^\infty\frac{d\bar{u}}{\pi}\frac{\rho_{tu}^{(n)}(\bar{t},\bar{u})}{(t-\bar{t})(u-\bar{u})}\\&+\int_0^\infty\frac{d\bar{s}}{\pi}\int_0^\infty\frac{d\bar{u}}{\pi}\frac{\rho_{su}^{(n)}(\bar{s},\bar{u})}{(s-\bar{s})(u-\bar{u})}, \end{aligned} \quad (5)$$

as can be confirmed in perturbation theory. In effective field theory applications, suitable subtractions may be required. In this work we focus on the contributions defined by the t- and u-channel spectral weights $\rho_t^{(n)}(\bar{t})$ and $\rho_u^{(n)}(\bar{u})$. They give rise to so-called left-hand cuts in the partial-wave scattering amplitudes. The s-channel contribution $\rho_s^{(n)}(\bar{s})$ gives rise to s-channel unitarity cuts which are referred to as right-hand cuts.

In a first step we will establish a spectral representation for a generic t-channel and u-channel term as shown in Fig. 1,

$$\int_{-1}^{1} dx \frac{\lambda_n(s,x)}{t[s,x]-m_t^2} = \sum_{i=\pm}\int_{-\infty}^{\infty}\frac{dm^2}{\pi}\frac{\varrho_{n,i}^{(t)}(m^2,m_t^2)}{s-c_i^{(t)}(m^2)} \times\left(\frac{d}{dm^2}c_i^{(t)}(m^2)\right),$$
$$\int_{-1}^{1} dx \frac{\lambda_n(s,x)}{u[s,x]-m_u^2} = \sum_{i=\pm}\int_{-\infty}^{\infty}\frac{dm^2}{\pi}\frac{\varrho_{n,i}^{(u)}(m^2,m_u^2)}{s-c_i^{(u)}(m^2)} \times\left(\frac{d}{dm^2}c_i^{(u)}(m^2)\right), \quad (6)$$

with the appropriate contour functions $c_\pm^{(t)}(m^2)$ and $c_\pm^{(u)}(m^2)$ that identify the location of the branch cuts and some properly constructed spectral weights $\varrho_{n,\pm}^{(t)}(m^2,m_t^2)$ and $\varrho_{n,\pm}^{(u)}(m^2,m_u^2)$. Given such a representations (6) the general result for a partial-wave projected distributed t-channel or u-channel exchange as given in (5) in terms of $\rho_t^{(n)}(\bar{t})$ and $\rho_u^{(n)}(\bar{u})$ is readily obtained in terms of the folded spectral weights

$$\varrho_{n,\pm}^{(t)}(m^2) = \int_0^\infty \frac{d\bar{t}}{\pi}\rho_t^{(n)}(\bar{t})\varrho_{n,\pm}^{(t)}(m^2,\bar{t}),$$
$$\varrho_{n,\pm}^{(u)}(m^2) = \int_0^\infty \frac{d\bar{u}}{\pi}\rho_u^{(n)}(\bar{u})\varrho_{n,\pm}^{(u)}(m^2,\bar{u}). \quad (7)$$

We note that a partial cancellation of the $+$ and $-$ contour contributions in (6) may occur whenever the two contours run along identical regions on the real axis.

While the derivation of the spectral weights $\varrho_{n,\pm}^{(t)}(m^2,t)$ and $\varrho_{n,\pm}^{(u)}(m^2,u)$ is quite cumbersome the identification of the contour functions $c_\pm^{(t)}(m^2)$ and $c_\pm^{(u)}(m^2)$ is straightforward. Owing to the Landau equations any possible branch point of a partial-wave amplitude must be associated with an endpoint singularity of the projection integral (4). Note that this is so only if the invariant amplitudes $F_n(s,t,u)$ are free of kinematical constraints. In the presence of kinematical constraints the functions $\lambda_n(s,x)$ may be singular at specific conditions which may lead to additional and unphysical branch points. In our case, the contour function may be introduced by the condition

$$u[c_\pm^{(u)}(m^2),\pm 1] = m^2, \qquad t[c_\pm^{(t)}(m^2),\pm 1] = m^2. \quad (8)$$

A few comments on the representation (6) are in order. The integral on the left-hand side of (6) defines an analytic function in s with branch points at $s=0$ and $s=c_\pm^{(u)}(m_u)$. Here we assume that the x-integration contour in (4) is appropriately deformed into the complex plane to avoid the situation $u[s,x]=m_u^2$ or $t[s,x]=m_t^2$ with $x\neq\pm 1$. It is convenient, though not mandatory, to define the branch cuts connected to the endpoint singularities of (6), i.e. the points $c_\pm^{(t)}(m_t^2)$ or $c_\pm^{(u)}(m_u^2)$, to lie on the lines defined by the functions $c_\pm^{(t)}(m^2)$ and $c_\pm^{(u)}(m^2)$. This procedure has the advantage that t- and u-channel processes with different exchange masses define branch cuts that are maximally overlapping. This is exploited in (7).

The right-hand sides of (6) may require a slight modification if the contour function $c_\pm^{(t)}(m^2)$ or $c_\pm^{(u)}(m^2)$ hits a threshold point $s=(m_a\pm M_a)^2$ or $(m_b\pm M_b)^2$ at a critical value $m_{\rm crit}$. Such a need reflects the possible presence of an anomalous threshold [21,44,45]. In this case the contour has to be deformed close to $m_{\rm crit}$. For instance, one may use a semicircle of radius ϵ centered around $m_{\rm crit}$.

III. SPECTRAL REPRESENTATION: GENERAL RESULTS

The contour functions $c_\pm^{(t)}(m^2)$ and $c_\pm^{(u)}(m^2)$ depend on the masses of initial and final particles for which we use the convenient notation

$$q^2=m_b^2, \qquad \bar{q}^2=m_a^2,$$
$$p^2=M_b^2, \qquad \bar{p}^2=M_a^2. \quad (9)$$

The root equations (8) for the contour functions can be solved analytically with the well- known result

$$c_{\pm,ab}^{(u)}(m^2) = \frac{1}{2}(M_a^2+m_a^2+M_b^2+m_b^2-m^2) + \frac{M_a^2-m_b^2}{\sqrt{2}m}\frac{M_b^2-m_a^2}{\sqrt{2}m} \pm\frac{m^2}{2}\sqrt{\left(1-2\frac{M_a^2+m_b^2}{m^2}+\frac{(M_a^2-m_b^2)^2}{m^4}\right)\left(1-2\frac{M_b^2+m_a^2}{m^2}+\frac{(M_b^2-m_a^2)^2}{m^4}\right)},$$
$$c_{\pm,ab}^{(t)}(m^2) = \frac{1}{2}(M_a^2+m_a^2+M_b^2+m_b^2-m^2) - \frac{M_a^2-M_b^2}{\sqrt{2}m}\frac{m_a^2-m_b^2}{\sqrt{2}m} \pm\frac{m^2}{2}\sqrt{\left(1-2\frac{M_a^2+M_b^2}{m^2}+\frac{(M_a^2-M_b^2)^2}{m^4}\right)\left(1-2\frac{m_a^2+m_b^2}{m^2}+\frac{(m_a^2-m_b^2)^2}{m^4}\right)}. \quad (10)$$

The spectral weights $\varrho^{(t)}_{n,\pm}(m^2,t)$ and $\varrho^{(u)}_{n,\pm}(m^2,u)$ introduced in (6) factorize. This is a consequence of specific properties of the kinematical functions $\lambda_n(s,x)$. They may have singularities at the thresholds $s=(m_a\pm M_a)^2$ and $(m_b\pm M_b)^2$ only. However, the x dependence in $\lambda_n(s,x)$ is such that the integrals (6) are finite at $s=(m_a\pm M_a)^2$ and $(m_b\pm M_b)^2$, at least for sufficiently large m_t and m_u. It holds

$$\begin{aligned}
\varrho^{(t)}_{n,\pm}(m^2,m_t^2) &= \lambda_n(c^{(t)}_\pm(m^2),x^{(t)}_\pm(m^2))\varrho^{(t)}_\pm(m^2,m_t^2),\\
x^{(t)}_\pm(m^2) &= \left.\frac{2\omega_a(s)\omega_b(s)-m_a^2-m_b^2+m_t^2}{2p_a(s)p_b(s)}\right|_{s=c^{(t)}_\pm(m^2)},\\
\varrho^{(u)}_{n,\pm}(m^2,m_u^2) &= \lambda_n(c^{(u)}_\pm(m^2),x^{(u)}_\pm(m^2))\varrho^{(u)}_\pm(m^2,m_u^2),\\
x^{(u)}_\pm(m^2) &= \left.\frac{M_a^2+m_b^2-m_u^2-2E_a(s)\omega_b(s)}{2p_a(s)p_b(s)}\right|_{s=c^{(u)}_\pm(m^2)},
\end{aligned}\tag{11}$$

with

$$p_i(s)=\sqrt{\frac{(s-(m_i+M_i)^2)(s-(m_i-M_i)^2)}{4s}},$$
$$\omega_i(s)=\frac{s-M_i^2+m_i^2}{2\sqrt{s}},\qquad E_i(s)=\frac{s-m_i^2+M_i^2}{2\sqrt{s}}.\tag{12}$$

The derivation of the master weight functions $\varrho^{(u)}_\pm(m^2,m_u^2)$ and $\varrho^{(t)}_\pm(m^2,m_t^2)$ is of utmost importance for the present development but quite tedious for the general case (see e.g. [21,46,47]). The authors did not find explicit expressions in the published literature for the general case. We present and discuss first the simple case where the u-channel and t-channel exchange masses m_u and m_t are sufficiently large. In this case the following results are readily established:

$$\varrho^{(t)}_\pm(m^2,m_t^2)=\begin{cases}-\pi\left.\frac{\Theta[m^2-m_t^2]}{2p_a(s)p_b(s)}\right|_{s=c^{(t)}_\pm(m^2)} & \text{for } \mathrm{Min}\{t_I^{(a)},t_I^{(b)}\}\le 0\\ \pm\pi\left.\frac{\Theta[m^2-m_t^2]}{2p_a(s)p_b(s)}\right|_{s=c^{(t)}_\pm(m^2)} & \text{for } \mathrm{Min}\{t_I^{(a)},t_I^{(b)}\}> 0\end{cases},$$
$$t_I^{(a)}=\frac{-M_a^2m_b^2+m_a^2M_b^2}{m_a^2-M_a^2},\qquad t_I^{(b)}=\frac{M_a^2m_b^2-m_a^2M_b^2}{m_b^2-M_b^2}.\tag{13}$$

While the form of the spectral weight is quite simple and intuitive, its associated phase factor is complicated, reflecting the choices of various Riemann sheets. We follow here a pragmatic approach. We will not give complicated arguments about which Riemann sheets to choose; rather, we present the final answer and assure that (6) was verified by numerical simulations for sufficiently large energies. It is worth pointing out that (13) holds for arbitrarily small exchange masses for the limiting case $m_a=m_b$ and $M_a=M_b$ with $t_I^{(a)}=t_I^{(b)}=0$.

The particular values $t_I^{(a)}$ and $t_I^{(b)}$ are determined by the conditions

$$\begin{aligned}
&\mathrm{Im}p_a^2c^{(t)}_\pm(m^2)=0 \quad\&\quad \mathrm{Im}c^{(t)}_\pm(m^2)\neq 0\to m^2=t_I^{(a)},\\
&\mathrm{Im}p_b^2c^{(t)}_\pm(m^2)=0 \quad\&\quad \mathrm{Im}c^{(t)}_\pm(m^2)\neq 0\to m^2=t_I^{(b)},
\end{aligned}\tag{14}$$

where we assure the independence of the solutions with respect to the contour indices $\pm$.

Before proceeding with a discussion of the more general case with an arbitrarily small exchange mass m_t, we provide the analogous result for the u-channel term:

$$\varrho^{(u)}_\pm(m^2,m_u^2)=\begin{cases}-\pi\left.\frac{\Theta[m^2-m_u^2]}{2p_a(s)p_b(s)}\right|_{s=c^{(u)}_\pm(m^2)} & \text{for } \mathrm{Min}\{u_I^{(a)},u_I^{(b)}\}\le 0\\ \pm\pi\left.\frac{\Theta[m^2-m_u^2]}{2p_a(s)p_b(s)}\right|_{s=c^{(u)}_\pm(m^2)} & \text{for } \mathrm{Min}\{u_I^{(a)},u_I^{(b)}\}> 0\end{cases},$$
$$u_I^{(a)}=\frac{-M_a^2M_b^2+m_a^2m_b^2}{m_a^2-M_a^2},\qquad u_I^{(b)}=\frac{-M_a^2M_b^2+m_a^2m_b^2}{m_b^2-M_b^2},\tag{15}$$

with

$$\begin{aligned}
&\mathrm{Im}p_a^2c^{(u)}_\pm(m^2)=0 \quad\&\quad \mathrm{Im}c^{(u)}_\pm(m^2)\neq 0\to m^2=u_I^{(a)},\\
&\mathrm{Im}p_b^2c^{(u)}_\pm(m^2)=0 \quad\&\quad \mathrm{Im}c^{(u)}_\pm(m^2)\neq 0\to m^2=u_I^{(b)}.
\end{aligned}\tag{16}$$

In (15) we assume m_u to be sufficiently large. Note the formal similarity of the expressions for the contour functions $c_\pm^{(u)}(m^2)$ and $c_\pm^{(t)}(m^2)$ as given in (10): applying $m_b \leftrightarrow M_b$ transforms the expressions into each other.

We turn to the general case with arbitrary exchange masses. It suffices to provide explicit expressions for the t-channel case. Corresponding expressions valid for the u-channel term follow by the replacement $m_b \leftrightarrow M_b$.

In a first step, we identify the points where a change of Riemann sheets, and therewith a phase change, may be required. All together there are 15 critical values for the squared exchange mass m_t^2. The expression (13) is valid for m_t^2 larger than the maximum of those 15 values. Two points $t_I^{(a)}$ and $t_I^{(b)}$ we encountered already in (13) and (14). An additional four points are determined by the conditions that the squared contour functions pass through the threshold points $(m_a \pm M_a)^2$ and $(m_b \pm M_b)^2$. It is intuitive that the latter are associated with a change of Riemann sheets and, therefore, will possibly cause a phase change of the spectral weight at such points. We introduce

$$\begin{aligned} t_+^{(a)} &= \frac{m_a M_b^2 + m_b^2 M_a}{m_a + M_a} - m_a M_a, \\ t_+^{(b)} &= \frac{m_b M_a^2 + m_a^2 M_b}{m_b + M_b} - m_b M_b, \\ c_\pm^{(t)}(m^2) &= (m_a + M_a)^2 \to m^2 = t_+^{(a)}, \\ c_\pm^{(t)}(m^2) &= (m_b + M_b)^2 \to m^2 = t_+^{(b)}, \end{aligned} \tag{17}$$

and

$$\begin{aligned} t_-^{(a)} &= \frac{m_a M_b^2 - m_b^2 M_a}{m_a - M_a} + m_a M_a, \\ t_-^{(b)} &= \frac{m_b M_a^2 - m_a^2 M_b}{m_b - M_b} + m_b M_b, \\ c_\pm^{(t)}(m^2) &= (m_a - M_a)^2 \to m^2 = t_-^{(a)}, \\ c_\pm^{(t)}(m^2) &= (m_b - M_b)^2 \to m^2 = t_-^{(b)}, \end{aligned} \tag{18}$$

where a solution exists either with respect to the subscript $\pm \to +$ or $\pm \to -$ depending on the specifics of case. The $c_+^{(t)}(m^2)$ contour runs through two threshold points at most. The same holds for the $c_-^{(t)}(m^2)$ contour: it may intersect the two threshold points that are avoided by $c_+^{(t)}(m^2)$.

Four further critical points are determined by the condition that the imaginary parts of the squared contour functions approach zero: the argument of the square root in (10) must vanish:

$$\begin{aligned} &m_\pm^2 = (m_a \pm m_b)^2, \qquad M_\pm^2 = (M_a \pm M_b)^2. \\ &v_\pm^+ = \mathrm{Max}\{m_\pm^2, M_\pm^2\}, \qquad v_\pm^- = \mathrm{Min}\{m_\pm^2, M_\pm^2\}. \end{aligned} \tag{19}$$

The critical values (19) determine whether the squared contour functions lie on the real axis or invade the complex plane. The latter holds for

$$\begin{matrix} v_+^- < m^2 < v_+^+ \\ v_-^- < m^2 < v_-^+ \end{matrix} \leftrightarrow \mathrm{Im} c_\pm^{(t)}(m^2) \neq 0 \quad \text{if } v_+^- > v_-^+ \tag{20}$$

and

$$\begin{matrix} v_-^+ < m^2 < v_+^+ \\ v_-^- < m^2 < v_+^- \end{matrix} \leftrightarrow \mathrm{Im} c_\pm^{(t)}(m^2) \neq 0 \quad \text{if } v_+^- < v_-^+. \tag{21}$$

The points m_+ and M_+ have a direct physical interpretation: for $m_t > m_+$ or $m_t > M_+$ the t-channel exchange particle turns unstable. Similarly, the critical points m_- and M_- reflect the opening of decay channels of initial or final particles.

In order to derive the generalization of (13), it is important to study the position of the critical points $v_\pm^+$ and $v_\pm^-$ in relation to the points $t_I^{(a)}$ and $t_I^{(b)}$ introduced already in (13). We derive the inequalities

$$\begin{aligned} &v_-^- < t_I^- < v_+^- \quad \& \quad t_I^+ > v_-^+ \quad \text{for } t_I^- > 0, \\ &\qquad\qquad\qquad\quad t_I^+ < v_+^- \quad \text{for } t_I^- < 0, \\ &t_I^+ = \mathrm{Max}\{t_I^{(a)}, t_I^{(b)}\}, \qquad t_I^- = \mathrm{Min}\{t_I^{(a)}, t_I^{(b)}\}, \end{aligned} \tag{22}$$

which follow with ease from the two identities

$$\begin{aligned} t_I^{(a)} &= M_b^2 + \frac{t_I^{(a)}}{t_I^{(b)}} M_a^2 = m_b^2 + \frac{t_I^{(a)}}{t_I^{(b)}} m_a^2, \\ t_I^{(b)} &= M_a^2 + \frac{t_I^{(b)}}{t_I^{(a)}} M_b^2 = m_a^2 + \frac{t_I^{(b)}}{t_I^{(a)}} m_b^2. \end{aligned} \tag{23}$$

It is useful to work out also the relative positions of the remaining critical points. After tedious considerations, we find the relations

$$\begin{aligned} t_+^- &\le v_-^- \le \mathrm{Min}\{v_-^+, v_+^-\} \le \mathrm{Min}\{t_+^+, t_-^-\} \\ &\le \mathrm{Max}\{t_+^+, t_-^-\} \le \mathrm{Max}\{v_-^+, v_+^-\} \\ &\le v_+^+ \le t_-^+ \quad \text{for } t_-^- > \mathrm{Min}\{v_-^+, v_+^-\}, \\ t_+^- &\le v_-^- \le \mathrm{Min}\{v_-^+, v_+^-\} \le \mathrm{Min}\{t_+^+, t_-^+\} \\ &\le \mathrm{Max}\{t_+^+, t_-^+\} \le \mathrm{Max}\{v_-^+, v_+^-\} \\ &\le v_+^+ \quad \text{for } t_-^- \le \mathrm{Min}\{v_-^+, v_+^-\}, \end{aligned} \tag{24}$$

where we introduced the notation

$$t_\pm^+ = \mathrm{Max}\{t_\pm^{(a)}, t_\pm^{(b)}\}, \qquad t_\pm^- = \mathrm{Min}\{t_\pm^{(a)}, t_\pm^{(b)}\}. \tag{25}$$

We are now prepared to display the master spectral weight, where we assume $m_a \neq m_b$ or $M_a \neq M_b$ in the following. Recall that for the diagonal limit with $m_a = m_b$ and $M_a = M_b$, the spectral weight is given by (13). We discriminate four different cases,

$$\varrho^{(t)}_{\pm}(m^2,m_t^2) = \begin{cases} \varrho^{(t)}_{\pm,1}(m^2,m_t^2) & \text{for } t_I^- \le 0 \quad \& \quad v_-^+ < v_+^- \\ \varrho^{(t)}_{\pm,2}(m^2,m_t^2) & \text{for } t_I^- > 0 \quad \& \quad v_-^+ < v_+^- \\ \varrho^{(t)}_{\pm,3}(m^2,m_t^2) & \text{for } t_I^- \le 0 \quad \& \quad v_-^+ \ge v_+^- \\ \varrho^{(t)}_{\pm,4}(m^2,m_t^2) & \text{for } t_I^- > 0 \quad \& \quad v_-^+ \ge v_+^- \end{cases},$$

$$\varrho^{(t)}_{\pm,i}(m^2,m_t^2) = \varrho^{(t)}_{\pm,i}(m)\Theta[m^2-m_t^2], \tag{26}$$

with

$$\begin{aligned}
\varrho^{(t)}_{\pm,1}(m^2) &= \frac{\pi}{2p_a(s)p_b(s)}\bigg|_{s=c^{(t)}_{\pm}(m^2)} \{-1+2\Theta[v_+^+-m^2]-2\Theta[v_+^--m^2]-2\Theta[v_-^+-m^2]\Theta[v_-^+-t_I^+] \\
&\quad +2\Theta[v_-^--m^2]\Theta[v_-^--t_I^+]+2\Theta[t_I^+-m^2]\Theta[t_I^+-v_-^-]\Theta[v_-^+-t_I^+]+2\Theta[t_\pm^+-m^2]-2\Theta[t_\mp^--m^2]\}, \\
\varrho^{(t)}_{\pm,2}(m^2) &= \frac{\pi}{2p_a(s)p_b(s)}\bigg|_{s=c^{(t)}_{\pm}(m^2)} \{\pm 1+2\Theta[v_+^+-m^2]\Theta[t_I^+-v_+^+]-2\Theta[v_+^--m^2]\Theta[t_I^+-v_+^-] \\
&\quad +2\Theta[t_I^+-m^2]\Theta[t_I^+-v_+^-]\Theta[v_+^+-t_I^+]-2\Theta[v_-^+-m^2]\Theta[v_-^+-t_I^-]+2\Theta[v_-^--m^2]\Theta[v_-^--t_I^-] \\
&\quad +2\Theta[t_I^--m^2]\Theta[t_I^--v_-^-]\Theta[v_-^+-t_I^-]+2\Theta[t_\pm^+-m^2]-2\Theta[t_\mp^\pm-m^2]\}, \\
\varrho^{(t)}_{\pm,3}(m^2) &= \frac{\pi}{2p_a(s)p_b(s)}\bigg|_{s=c^{(t)}_{\pm}(m^2)} \{-1+2\Theta[v_+^+-m^2]+2\Theta[v_-^--m^2]\Theta[v_-^--t_I^+] \\
&\quad +2\Theta[t_I^+-m^2]\Theta[t_I^+-v_-^-]-2\Theta[t_\mp^\pm-m^2]-2\Theta[t_\mp^--m^2]\}, \\
\varrho^{(t)}_{\pm,4}(m^2) &= \frac{\pi}{2p_a(s)p_b(s)}\bigg|_{s=c^{(t)}_{\pm}(m^2)} \{\pm 1+2\Theta[v_+^+-m^2]\Theta[t_I^+-v_+^+]+2\Theta[t_I^+-m^2]\Theta[v_+^+-t_I^+] \\
&\quad +2\Theta[t_I^--m^2]\Theta[t_I^--v_-^-]-2\Theta[t_\mp^\pm-m^2]-2\Theta[t_\mp^--m^2]\},
\end{aligned} \tag{27}$$

where we apply the convenient notations (19), (22), and (25). The result (27) deserves some discussion. The first term in each of the four expressions in (27) describes the opening of a normal left-hand cut at $m^2 > m_t^2$. While the conditions $m^2 > v_-^\pm$ characterize the opening of decay channels of the exchanged particle the conditions $m^2 < v_+^\pm$ signal an unstable initial or final state. Anomalous thresholds open at $m^2 < t_\pm^+$ or $m^2 < t_\pm^-$. With (27) we also specify implicitly which contour runs through which threshold points. This follows since each threshold point is associated with a sign change of the spectral functions as detailed in (27) at $m^2 = t_\pm^+$ or $m^2 = t_\pm^-$. For a given plus or minus contour and a selected case $i = 1,\ldots,4$ in (26), two critical values out of the four $t_\pm^+$ and $t_\pm^-$ points are selected unambiguously.

The merit of (27) lies in its generality. It is a convenient starting point for coupled-channel studies with many channels involved, where a case-by-case study is prohibitive. In certain cases the result (27) may be further simplified by the observation that there may be partial cancellations of the plus and minus contour contributions in regions where they are moving on the real axis. With (27) it is straightforward to implement such cancellations in a computer code.

We alert the reader that the result (27) requires an analytic continuation for the case that a channel with nonzero angular momentum $L \neq 0$ is considered. This implies that the functions $\lambda_n(s,x)$ in (6) are singular at thresholds and consequently the contour function $c^{(t)}_\pm(m^2)$ needs to be deformed into the complex m^2 plane close to the critical values $m^2_{\rm crit} = t_\pm^+$ and $t_\pm^-$. Using semicircles centered around the critical points this is readily achieved. The spectral weight is continued onto the deformed contour by the condition that it is continuous along the semicircles. This leads to an unambiguous definition of the Θ functions in (27) along the deformed contour: Θ functions in the phase parameters of the semicircles arise. Since the analytic expression for the critical phases are quite complicated and implicit they may be determined numerically.

The spectral weights in (27) are constructed such that the representation (6) holds for sufficiently large s. It does not necessarily hold for arbitrarily small energies. For the specific case with $m_t^2 < t_+^-$ the contour function cuts through the larger threshold point

$$c^{(t)}_{-,ab}(m^2) = \mathrm{Max}\{(m_a+M_a)^2,(m_b+M_b)^2\} \quad \text{with} \quad m^2 = t_+^-, \tag{28}$$

and (6) is not realized for energies slightly above that larger threshold. An analytic continuation of the rhs of (6) is possible to affirm the realization of (6) at the larger threshold and above. We specify the analytic continuation by additional terms $\Delta\varrho^{(t-)}_{\pm,i}(m^2 m_t^2)$ in (27). Replacing the spectral weight in (11) and (26) by

$$\varrho^{(t)}_{\pm,i}(m^2,m_t^2) = \varrho^{(t)}_{\pm,i}(m^2)\Theta[m^2-m_t^2] + \Delta\varrho^{(t-)}_{\pm,i}(m^2,m_t^2), \tag{29}$$

will insure the validity of (6) for energies exceeding the larger threshold point.

The construction of $\Delta\varrho^{(t-)}_{\pm,i}(m^2,m_t^2)$ requires a further set of specific contour points as conveniently introduced by the condition

$$c^{(t)}_{\pm}((m_a\pm m_b)^2) = c^{(t)}_{\pm}(\bar m^2_{\pm}),$$
$$c^{(t)}_{\pm}((M_a\pm M_b)^2) = c^{(t)}_{\pm}(\bar M^2_{\pm}), \tag{30}$$

where we are interested in the solutions with $\bar m^2_{\pm} \neq (m_a \pm m_b)^2$ and $\bar M^2_{\pm} \neq (M_a \pm M_b)^2$. The latter determine exchange masses where the contour function returns to itself. We derive the explicit formulae

$$\bar m^2_{\pm} = m_a^2 \mp \frac{m_b}{m_a}M_a^2 + m_b(m_b \mp m_a)\frac{M_a^2-M_b^2}{m_a^2-m_b^2} - \frac{m_b}{m_a}\frac{(m_b\pm m_a)(m_a^2-M_a^2)^2}{m_b(m_a m_b \pm (m_a^2-M_a^2)) - m_a M_b^2},$$
$$\bar M^2_{\pm} = M_a^2 \mp \frac{M_b}{M_a}m_a^2 + M_b(M_b \mp M_a)\frac{m_a^2-m_b^2}{M_a^2-M_b^2} - \frac{M_b}{M_a}\frac{(M_b\pm M_a)(M_a^2-m_a^2)^2}{M_b(M_a M_b \pm (M_a^2-m_a^2)) - M_a m_b^2},$$
$$\{\bar v_{\pm}^-,\bar v_{\pm}^+\} = \begin{cases} \{\bar m^2_{\pm},\bar M^2_{\pm}\} & \text{if } (m_a\pm m_b)^2 < (M_a\pm M_b)^2 \\ \{\bar M^2_{\pm},\bar m^2_{\pm}\} & \text{if } (m_a\pm m_b)^2 > (M_a\pm M_b)^2 \end{cases}, \tag{31}$$

and introduce further notations $\bar v_{\pm}^-$ and $\bar v_{\pm}^+$. While the points $v_{\pm}^+$ and $v_{\pm}^-$ characterize the exchange masses where the contour leaves the real axis and invades the complex plane, the associated points $\bar v_{\pm}^-$ and $\bar v_{\pm}^+$ determine where the contour returns to those exit points possibly. It is important to know the relative locations of the points $\bar v_{\pm}^+$ and $\bar v_{\pm}^-$ with respect to the critical points introduced before.

We first focus on the relevant case with $t_+^- > 0$ for which we derive the following relations

$$\begin{aligned}
&t_+^- > 0 \to \bar v_-^- \le t_+^- \le v_-^- && \text{always},\\
&t_-^- \le 0 \quad \& \quad v_-^+ \le t_+^+ \le \bar v_-^+ \le \mathrm{Min}\{v_+^-,t_-^+\} && \text{if } t_I^- \le 0 \quad \& \quad v_-^+ < v_+^-,\\
&v_-^+ \le t_+^+ \le \bar v_-^+ \le \mathrm{Min}\{v_+^-,t_-^-\} \le t_-^+ && \text{if } t_I^- > 0 \quad \& \quad v_-^+ < v_+^-,\\
&t_-^- \le 0 \quad \& \quad v_+^- \le t_-^+ \le \bar v_+^- \le \mathrm{Min}\{v_-^+,t_+^+\} && \text{if } t_I^- \le 0 \quad \& \quad v_-^+ \ge v_+^-,\\
&v_+^- \le t_-^- \le \bar v_+^- \le \mathrm{Min}\{v_-^+,t_+^+\} \le t_-^+ && \text{if } t_I^- > 0 \quad \& \quad v_-^+ \ge v_+^-.
\end{aligned} \tag{32}$$

The analytic continuation of the rhs of (6) is introduced upon the identification of an appropriate closed contour, inside which the spectral weight is analytic. For an energy outside that closed domain the dispersion integral of (6), considered with respect to that closed contour, is unchanged. For s inside the closed domain it is altered necessarily. The closed contour needed for the desired analytic continuation is readily identified with

$$c^{(t)}_{-,ab}(m^2) \quad \text{with} \quad \bar v_-^- < m^2 < \begin{cases} v_-^+ & \text{if } v_-^+ < v_+^- \\ v_+^- & \text{if } v_+^- < v_-^+ \end{cases},$$
$$c^{(t)}_{+,ab}(m^2) \quad \text{with} \quad v_-^- < m^2 < \begin{cases} \bar v_-^+ & \text{if } v_-^+ < v_+^- \\ \bar v_+^- & \text{if } v_+^- < v_-^+ \end{cases}, \tag{33}$$

where a closed domain arises upon the union of the plus and minus contour lines introduced in (33). The spectral weights $\Delta\varrho^{(t-)}_{\pm,i}(m^2,m_t^2)$ in (29) follow from the condition that the expressions (29) vanish for exchange masses $m > m_t$ on the closed contour as introduced in (33). If the contour cuts through the largest threshold point and the spectral weight would be nonvanishing in this region a singular threshold behavior would arise necessarily from the rhs of (6). This would contradict the lhs of (6), which implies a regular behavior at the largest threshold point always. The situation is reconciled by the analytic continuation we are after. We find the result

$$\Delta\varrho^{(t-)}_{\pm,1}(m^2,m_t^2)=\pi\frac{\Theta[t_+^- -m_t^2]}{2p_a(s)p_b(s)}\Big|_{s=c^{(t)}_\pm(m^2)}\times\{(2\Theta[m^2-t_I^+]\Theta[v_-^+-t_I^+]-1)\Theta[m^2-v_-^-]\Theta[v_-^+-m^2]+(1-2\Theta[\pm t_+^\pm\mp m^2])\Theta[\pm\bar v_-^\pm\mp m^2]\Theta[\pm m^2\mp v_-^\pm]\},$$

$$\Delta\varrho^{(t-)}_{\pm,2}(m^2,m_t^2)=\pi\frac{\Theta[t_+^- -m_t^2]}{2p_a(s)p_b(s)}\Big|_{s=c^{(t)}_\pm(m^2)}\times\{(2\Theta[m^2-t_I^-]\Theta[v_-^+-t_I^-]-1)\Theta[m^2-v_-^-]\Theta[v_-^+-m^2]+(1-2\Theta[\pm t_+^\pm\mp m^2])\Theta[\pm\bar v_-^\pm\mp m^2]\Theta[\pm m^2\mp v_-^\pm]\},$$

$$\Delta\varrho^{(t-)}_{\pm,3}(m^2,m_t^2)=\pi\frac{\Theta[t_+^- -m_t^2]}{2p_a(s)p_b(s)}\Big|_{s=c^{(t)}_\pm(m^2)}\times\{(1-2\Theta[t_I^+-m^2])\Theta[m^2-v_-^-]\Theta[v_+^- -m^2]+(1-2\Theta[m^2-t_\mp^\pm])\Theta[\pm\bar v_\pm^-\mp m^2]\Theta[\pm m^2\mp v_\pm^-]\},$$

$$\Delta\varrho^{(t-)}_{\pm,4}(m^2,m_t^2)=\pi\frac{\Theta[t_+^- -m_t^2]}{2p_a(s)p_b(s)}\Big|_{s=c^{(t)}_\pm(m^2)}\times\{(1-2\Theta[t_I^--m^2])\Theta[m^2-v_-^-]\Theta[v_+^- -m^2]+(1-2\Theta[m^2-t_\mp^-])\Theta[\pm\bar v_\pm^-\mp m^2]\Theta[\pm m^2\mp v_\pm^-]\}. \quad (34)$$

Due to the particular construction of $\Delta\varrho^{(t-)}_{\pm,i}(m^2,m_t^2)$ it is possible to write the total spectral weights in (29) directly in terms of the functions $\varrho^{(t)}_{\pm,i}(m)$ introduced in (27). All together we affirm that using either (34) in (29) or

$$\varrho^{(t)}_{+,i}(m^2,m_t^2)=\{-\Theta[t_+^- -m_t^2]\Theta[m^2-v_-^-]\Theta[\bar v_-^+-m^2]+\Theta[m^2-m_t^2]\}\varrho^{(t)}_{+,i}(m)\quad\text{for } i=1,2,$$
$$\varrho^{(t)}_{+,i}(m^2,m_t^2)=\{-\Theta[t_+^- -m_t^2]\Theta[m^2-v_-^-]\Theta[\bar v_+^- -m^2]+\Theta[m^2-m_t^2]\}\varrho^{(t)}_{+,i}(m)\quad\text{for } i=3,4,$$
$$\varrho^{(t)}_{-,i}(m^2,m_t^2)=\{-\Theta[t_+^- -m_t^2]\Theta[m^2-\bar v_-^-]\Theta[\mathrm{Min}\{v_-^+,v_+^-\}-m^2]+\Theta[m^2-m_t^2]\}\varrho^{(t)}_{-,i}(m)\quad\text{for } i=1,2,3,4, \quad (35)$$

the validity of (6) for energies exceeding the larger threshold point is ensured.

There is a further complication to be addressed. The representation (6) is not necessarily valid for energies in between the two normal thresholds

$$\mathrm{Min}\{m_a+M_a,m_b+M_b\}<\sqrt{s}<\mathrm{Max}\{m_a+M_a,m_b+M_b\}. \quad (36)$$

Two cases need to be discriminated. Either both pseudothreshold values, $|m_a-M_a|$ and $|m_b-M_b|$ are smaller than the two normal thresholds m_a+M_a and m_b+M_b or this is not true. In both cases an analytic continuation of the lhs of (6), may be required. For the case of an inverted threshold order with e.g.

$$|m_b-M_b|\le m_b+M_b\le|m_a-M_a|\le m_a+M_a, \quad (37)$$

also the rhs of (6) needs an analytic continuation for energies below the larger pseudothreshold energy. Such an inversion occurs always for $i=3$ or $i=4$ with $v_-^+\ge v_+^-$ but is impossible for $i=1$ or $i=2$ in (26).

We first construct the analytic continuation of the lhs (6), which is necessary provided that the following condition is realized

$$\mathrm{Max}\{(m_a-M_a)^2,(m_b+M_b)^2\}<s_+(m_t^2)<(m_a+M_a)^2$$
$$\text{or}\quad \mathrm{Max}\{(m_a-M_a)^2,(m_b+M_b)^2\}<s_-(m_t^2)<(m_a+M_a)^2,$$
$$s_\pm(m_t^2)=\frac{m_a^2+M_a^2+m_b^2+M_b^2}{2}-m_t^2\pm\sqrt{\left(\frac{m_a^2+M_a^2+m_b^2+M_b^2}{2}-m_t^2\right)^2-(M_a^2-m_a^2)(M_b^2-m_b^2)}, \quad (38)$$

where we assumed $m_a + M_a \geq m_b + M_b$ without loss of generality. The particular functions $s_\pm(m_t^2)$ introduced in (38) pass through the thresholds at the critical points $m_t^2 = t_\pm^{(a)}$ and $m_t^2 = t_\pm^{(b)}$ introduced in (17), (18) when studying the contour properties. We derive

$$\text{for } t_\pm^{(a)} \geq \frac{m_b^2 + M_b^2}{2} - \frac{m_a^2 + M_a^2}{2} \mp 2m_a M_a,$$
$$s_-(t_\pm^{(a)}) = (m_b^2 - M_b^2)\frac{m_a \mp M_a}{m_a \pm M_a} \leq s_+(t_\pm^{(a)}) = (m_a \pm M_a)^2, \tag{39}$$

where the role of s_+ and s_- is interchanged in the case that the first inequality in (39) is not realized. Corresponding results for $s_\pm(t_\pm^{(b)})$ follow from (39) by interchanging the indices $a \leftrightarrow b$.

The analytic continuation is achieved by deforming the x-integration contour: a complex contour $\gamma(z)$ with $\gamma(0) = -1$ and $\gamma(1) = 1$ needs to be devised accordingly. At sufficiently large s the representation (6) is true always by construction, only as one lowers the energy a deformation of the integration contour is required. We derive the result

$$\int_0^1 dz\gamma'(z)\frac{\lambda_n(s,\gamma(z))}{t[s,\gamma(z)] - m_t^2} = \int_{-1}^{+1} dx \frac{\lambda_n(s,x)}{t_{ab}(s) + 2xp_a(s)p_b(s)} - i\pi \frac{\lambda_n(s, -\frac{t_{ab}(s)}{2p_a(s)p_b(s)})}{p_a(s)p_b(s)}\Theta[\mathrm{Im}(t_{ab}(s)p_a(s)p_b(s))],$$
$$t[s,x] - m_t^2 = t_{ab}(s) + 2xp_a(s)p_b(s), \tag{40}$$

where we consider a typical t-channel process (see also [44,45]) and recall that the deformation of the x-integration contour is required only if the condition (38) is realized. The function $t_{ab}(s)$ is defined implicitly in (40). For s real the function $t_{ab}(s)$ is real as well. The analytic continuation (40) is valid for $\sqrt{s} > m_a + M_a$ and $\sqrt{s} > m_b + M_b$ at least. For smaller energies the expressions may demand further modifications. The continuation is necessary since the function $t_{ab}(s)$ may pass through zero while $\mathrm{Im}(p_a(s)p_b(s)) \neq 0$. This is the condition (38). If one dropped the second term in (40) the integral would be discontinuous right where $t_{ab}(s) = 0$. Such a discontinuity would be incompatible with the representation (6). Note that for the validity of (40) it is irrelevant which of the various normal or anomalous thresholds in (27) cause the occurrence of a zero in $t_{ab}(s)$: in any case the proper result must be continuous at that zero. A direct consequence of the analytic continuation is the presence of an anomalous threshold behavior: due to the second line of (40) the dispersion integral (6) may exhibit a singularity at a threshold or pseudothreshold energy [44,45].

It is left to derive the analytic continuation of the rhs (6) mandatory for (38). Using the deformed x-integration contour of (40) and replacing the spectral weight $\varrho_{\pm,i}^{(t)}(m^2, m_t^2)$ in (26) by

$$\varrho_{\pm,i}^{(t)}(m^2)\Theta[m^2 - m_t^2] + \Delta\varrho_{\pm,i}^{(t-)}(m^2, m_t^2) + \Delta\varrho_{\pm,i}^{(t+)}(m^2, m_t^2), \tag{41}$$

will ensure the validity of (6) for energies exceeding any of the two normal thresholds.

We consider first the case $t_I^- > 0$ with $i = 2$ or $i = 4$ in (41). In order to derive the analytic continuation it is useful to establish the inequalities

$$\begin{aligned} &t_I^- > 0 \to \bar{v}_+^+ \geq t_-^+ \geq v_+^+ \quad \text{or} \quad \bar{v}_+^+ < v_+^+, \\ &t_-^- \geq t_+^+ \quad \& \quad v_+^- \geq t_-^- \geq \bar{v}_+^- \geq \mathrm{Max}\{v_-^+, t_+^-\} \quad \text{if} \quad v_-^+ < v_+^-, \\ &t_+^+ \geq \quad \& \quad v_-^+ \geq t_+^+ \geq \bar{v}_-^+ \geq \mathrm{Max}\{v_+^-, t_+^-\} \quad \text{if} \quad v_-^+ \geq v_+^-, \end{aligned} \tag{42}$$

which suggest the application of the following closed contour

$$c_{+,ab}^{(t)}(m^2) \quad \text{with} \quad \mathrm{Max}\{\bar{v}_+^+, v_+^+\} > m^2 > \begin{cases} v_+^- & \text{if } v_-^+ < v_+^- \\ v_-^+ & \text{if } v_+^- < v_-^+ \end{cases},$$
$$c_{-,ab}^{(t)}(m^2) \quad \text{with} \quad v_+^+ > m^2 > \begin{cases} \bar{v}_+^- & \text{if } v_-^+ < v_+^- \\ \bar{v}_-^+ & \text{if } v_+^- < v_-^+ \end{cases}. \tag{43}$$

First, we assume $\bar{v}_+^+ \geq v_+^+$ for which the spectral weights $\Delta\varrho_{\pm,i}^{(t+)}(m^2, m_t^2)$ are constructed from the condition that the expression (41) vanishes for m lying on the contours (43). We find the result

$$\Delta\varrho^{(t+)}_{\pm,2}(m^2,m_t^2)=\pi\frac{\Theta[t_-^- - m_t^2]}{2p_a(s)p_b(s)}\Big|_{s=c^{(t)}_\pm(m^2)}$$
$$\times\{(1-2\Theta[t_I^+ - m^2]\Theta[t_I^+ - v_+^-])\Theta[m^2 - v_+^-]\Theta[v_+^+ - m^2]$$
$$+(2\Theta[\pm t_-^\pm \mp m^2]-1)\Theta[\pm\bar v_+^\pm \mp m^2]\Theta[\pm m^2 \mp v_+^\pm]\},$$
$$\Delta\varrho^{(t+)}_{\pm,4}(m^2,m_t^2)=\pi\frac{\Theta[t_+^+ - m_t^2]}{2p_a(s)p_b(s)}\Big|_{s=c^{(t)}_\pm(m^2)}$$
$$\times\{(2\Theta[m^2 - t_I^+]\Theta[v_+^+ - t_I^+]-1)\Theta[m^2 - v_-^+]\Theta[v_+^+ - m^2]$$
$$+(2\Theta[t_\mp^+ - m^2]-1)\Theta[\pm\bar v_\pm^+ \mp m^2]\Theta[\pm m^2 \mp v_\pm^+]\}. \quad (44)$$

For $\bar v_+^+ < v_+^+$ the analytic continuation requires yet the further critical point,

$$t_0=(M_a^2m_b^2-m_a^2M_b^2)\frac{m_a^2-M_a^2-m_b^2+M_b^2}{(m_a^2-M_a^2)(m_b^2-M_b^2)}, \quad (45)$$

which specifies the exchange mass where either the plus or the minus contour runs through the particular point $s=0$.

The appropriate closed contour defining the desired analytic continuation needs to be extended: while the minus contour specification in (43) remains untouched the plus contour must be enlarged as to include the region $v_+^+ \le m^2 \le \infty$. The results (44) are valid for both cases $\bar v_+^+ \le v_+^+$ and $\bar v_+^+ \ge v_+^+$ for masses m in the regions introduced in (43). On the extended plus contour the spectral weight is

$$\Delta\varrho^{(t+)}_{+,2}(m^2,m_t^2)=\pi\frac{\Theta[t_-^- - m_t^2]}{2p_a(s)p_b(s)}\Big|_{s=c^{(t)}_+(m^2)}\begin{cases}+2 & \text{for } v_+^+\le m^2\le t_0\\ +1 & \text{for } t_0\le m^2\le t_-^+\\ -1 & \text{for } t_-^+\le m^2\le\infty\end{cases},$$
$$\Delta\varrho^{(t+)}_{+,4}(m^2,m_t^2)=\pi\frac{\Theta[t_+^+ - m_t^2]}{2p_a(s)p_b(s)}\Big|_{s=c^{(t)}_+(m^2)}\begin{cases}+2 & \text{for } v_+^+\le m^2\le t_0\\ +1 & \text{for } t_0\le m^2\le t_-^+\\ -1 & \text{for } t_-^+\le m^2\le\infty\end{cases}, \quad (46)$$

for $\bar v_+^+ \le v_+^+ \le m^2 \le \infty$.

It is left to consider $t_I^- \le 0$ with $i=1$ or $i=3$ in (41). Four distinct cases arise which are characterized by the following inequalities

$$\begin{aligned}
&t_I^- \le 0 \to \bar v_+^+ \le v_+^+ && \text{always,}\\
&v_+^- \ge t_-^+ \ge \bar v_+^- \ge \mathrm{Max}\{v_-^+, t_+^-\} && \text{if} \quad t_+^+ \le t_-^+ \,\&\, v_-^+ < v_+^-,\\
&t_-^- \le t_0 \le \bar v_+^+ \le v_-^- &&\\
&v_-^+ \ge t_+^+ \ge \bar v_-^+ \ge \mathrm{Max}\{v_+^-, t_+^-\} && \text{if} \quad t_+^+ \ge t_-^+ \,\&\, v_-^+ \ge v_+^-,\\
&t_-^- \le t_0 \le \bar v_+^+ \le v_-^- &&\\
&v_-^+ \le t_-^+ \le \bar v_-^+ \le v_+^- \quad \& \quad t_+^- \le 0 && \text{if} \quad t_+^+ \ge t_-^+ \,\&\, v_-^+ < v_+^-,\\
&\bar v_-^- \ge v_-^- \quad \text{or} \quad \bar v_-^- \le t_-^- \le v_-^- &&\\
&v_+^- \le t_+^+ \le \bar v_+^- \le v_-^+ \quad \& \quad t_+^- \le 0 && \text{if} \quad t_+^+ \le t_-^+ \,\&\, v_-^+ \ge v_+^-.\\
&\bar v_-^- \ge v_-^- \quad \text{or} \quad \bar v_-^- \le t_-^- \le v_-^- &&
\end{aligned} \quad (47)$$

The first two cases in (47) lead to a closed contour similar to the one introduced in (43). While the mass range for the minus part in (43) is unchanged the plus part extends to arbitrarily large and negative m^2. It holds

$$m^2 \le \bar v_+^+ \quad \text{or} \quad v_+^+ > m^2 > \begin{cases} v_+^- & \text{if } v_-^+ < v_+^-\\ v_-^+ & \text{if } v_+^- < v_-^+\end{cases}. \quad (48)$$

The last two cases in (47) involve yet the further closed contour

$$c^{(t)}_{-,ab}(m^2) \quad \text{with} \quad v_-^- < m^2 < \begin{cases} \bar{v}_-^+ & \text{if } v_-^+ < v_+^- \\ \bar{v}_+^- & \text{if } v_+^- < v_-^+ \end{cases},$$
$$c^{(t)}_{+,ab}(m^2) \quad \text{with} \quad \text{Min}\{\bar{v}_-^-, v_-^-\} < m^2 < \begin{cases} v_-^+ & \text{if } v_-^+ < v_+^- \\ v_+^- & \text{if } v_+^- < v_-^+ \end{cases}. \tag{49}$$

For $\bar{v}_-^- \le v_-^-$ the spectral weights $\Delta\varrho^{(t+)}_{\pm,i}(m^2, m_t^2)$ with $i = 1$ and $i = 3$ follow from the requirement that the expressions (41) vanish for exchange masses m on the closed contour as specified in (43) or (49) depending on the specifics of the case. Some algebra leads to

$$\begin{aligned}
\Delta\varrho^{(t+)}_{\pm,1}(m^2, m_t^2) &= \pi \frac{\Theta[t_-^+ - m_t^2]}{2p_a(s)p_b(s)}\bigg|_{s=c^{(t)}_\pm(m^2)} \Theta[t_-^+ - t_+^+] \times \{-\Theta[m^2 - v_+^-]\Theta[v_+^+ - m^2] + (2\Theta[\mp m^2 \pm t_-^\mp] - 1 \\
&\quad - \Theta[\pm m^2 \mp t_0])\Theta[\pm\bar{v}_+^\pm \mp m^2]\Theta[v_+^\pm - m^2]\} + \pi \frac{\Theta[t_-^- - m_t^2]}{2p_a(s)p_b(s)}\bigg|_{s=c^{(t)}_\pm(m^2)} \Theta[t_+^+ - t_-^+] \\
&\quad \times \{(2\Theta[m^2 - t_I^+]\Theta[v_-^+ - t_I^+] - 1)\Theta[m^2 - v_-^-]\Theta[v_-^+ - m^2] \\
&\quad + (2\Theta[\pm t_-^\mp \mp m^2] - 1)\Theta[\pm m^2 \mp \bar{v}_-^\mp]\Theta[\pm v_-^\mp \mp m^2]\}, \\
\Delta\varrho^{(t+)}_{\pm,3}(m^2, m_t^2) &= \pi \frac{\Theta[t_+^+ - m_t^2]}{2p_a(s)p_b(s)}\bigg|_{s=c^{(t)}_\pm(m^2)} \Theta[t_+^+ - t_-^+] \times \{-\Theta[m^2 - v_-^+]\Theta[v_+^+ - m^2] + (2\Theta[t_\mp^\mp - m^2] - 1 \\
&\quad - \Theta[\pm m^2 \mp t_0])\Theta[\pm\bar{v}_\pm^+ \mp m^2]\Theta[v_\pm^+ - m^2]\} + \pi \frac{\Theta[t_-^- - m_t^2]}{2p_a(s)p_b(s)}\bigg|_{s=c^{(t)}_\pm(m^2)} \Theta[t_-^+ - t_+^+] \\
&\quad \times \{(2\Theta[m^2 - t_I^+] - 1)\Theta[m^2 - v_-^-]\Theta[v_+^- - m^2] + (2\Theta[t_\mp^\mp - m^2] - 1)\Theta[\pm m^2 \mp \bar{v}_\mp^-]\Theta[\pm v_\mp^- \mp m^2]\}.
\end{aligned} \tag{50}$$

The results (50) are valid for both cases $\bar{v}_-^- \le v_-^-$ and $\bar{v}_-^- \ge v_-^-$ for masses m in the regions introduced in (43) and (49). A generalization is needed if the contour (49) is probed with $\bar{v}_-^- \ge v_-^-$. While the minus contour region is unchanged the plus contour of (49) is modified to cover the additional interval $t_-^- \le m^2 \le v_-^-$. On the extended plus contour the spectral weight is

$$\Delta\varrho^{(t+)}_{+,1}(m^2, m_t^2) = \pi \frac{\Theta[t_+^+ - t_-^+]}{2p_a(s)p_b(s)}\bigg|_{s=c^{(t)}_+(m^2)} \begin{cases} -2 & \text{for } t_-^- \le m^2 \le v_-^- \\ 0 & \text{for } m^2 \le t_-^- \end{cases},$$
$$\Delta\varrho^{(t+)}_{+,3}(m^2, m_t^2) = \pi \frac{\Theta[t_-^+ - t_+^+]}{2p_a(s)p_b(s)}\bigg|_{s=c^{(t)}_+(m^2)} \begin{cases} -2 & \text{for } t_-^- \le m^2 \le v_-^- \\ 0 & \text{for } m^2 \le t_-^- \end{cases}, \tag{51}$$

for $m^2 \le v_-^-$ and $m_t^2 \le t_-^-$.

IV. SPECTRAL REPRESENTATION: SOME EXAMPLES

In this section we illustrate the formalism developed above at hand of several selected reactions with specific contributions from t- and u-channel exchange processes. We pick reactions which give a good illustration of the various cases summarized in the general spectral density (27) and (41). In Fig. 2 and Fig. 5 our choices are shown. We consider five t-channel and five u-channel processes involving pseudoscalar and vector particles.

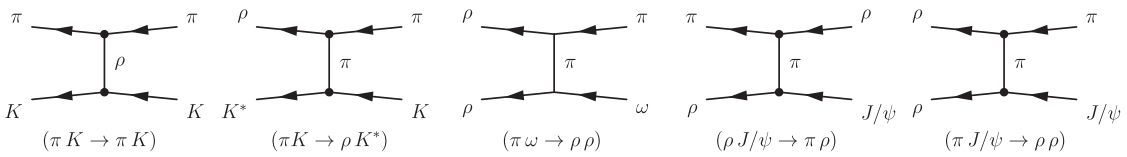

FIG. 2. Some specific t-channel exchange processes.

TABLE I. Critical points for the t-channel exchange processes shown in Fig. 2 in units m_π^2.

		$\pi K \to \pi K$	$\pi K \to \rho K^*$	$\pi\omega \to \rho\rho$	$\rho J/\psi \to \pi\rho$	$\pi J/\psi \to \rho\rho$
1	t_+^+	0	29.8812	25.4465	97.3278	221.066
2	t_-^+	0	30.5313	∞	116.185	∞
3	t_+^-	0	−29.6174	−14.5458	−118.153	8.67998
4	t_-^-	0	−36.8085	36.7849	−66.4585	53.5515
5	t_I^+	0	30.2063	∞	15.4347	∞
6	t_I^-	0	−33.2129	31.1157	−0.984286	31.1157
7	v_+^+	51.5765	101.333	126.503	784.778	784.778
8	v_-^+	0	20.9594	20.9594	284.179	284.179
9	v_+^-	4	43.2720	43.2720	43.2720	43.2720
10	v_-^-	0	8.32172	0.00829	20.9594	20.9594
11	$\bar{v}_+^+$	0	8.29860	−15.6877	20.3388	−118.153
12	$\bar{v}_-^+$	Indeterminate	43.2466	36.4702	43.8217	116.185
13	$\bar{v}_+^-$	0	20.9722	25.6933	279.869	97.3278
14	$\bar{v}_-^-$	Indeterminate	101.577	−1812.17	826.092	−66.4585
15	t_0	0	−3.00669	∞	14.4504	∞

In a first step we compute the list of critical exchange masses and collect them in Table I for the t-channel processes. For later convenience the critical points are labeled from 1 to 15. Isospin averaged particle masses from the Particle Data Group are used. All dimension full quantities are expressed in units of the isospin averaged pion masses. A critical exchange mass is not always active in the expression (27). Only if it is larger than the mass of the exchange particle it may turn relevant. The extra terms introduced in (41) imply a further analytic continuation of the dispersion integral (6). While the additional terms (34) are required for the validity of (6) slightly above the largest threshold point, the extra contributions (44), (50) are necessary to realize (6) in between the two nominal thresholds. In the absence of such terms (6) holds only for large s exceeding some critical value. All extra terms (34), (44), and (50) will be illustrated by our t-channel examples.

We briefly discuss the t-channel processes characterized by the list of critical exchange points Table I. For our first t-channel reaction $\pi K \to \pi K$ two critical points v_+^+ and v_+^-, which are number 7 and 9, may be relevant for both contour lines $c_+^{(t)}(m^2)$ and $c_-^{(t)}(m^2)$. Since the square of the exchange mass, the ρ-meson mass, is larger than v_+^-, there is only v_+^+ left. For this example it holds $t_I^- \leq 0$ and $v_-^+ < v_+^-$ so that the corresponding spectral weight is given by the first case in (27). The contour lines are shown in the center of Fig. 3. The two contours leave the real axis at $m^2 = v_+^-$. At the second critical point $m^2 = v_+^+$ the two contours return to the real axis. As a consequence, the spectral weight develops an imaginary part for $v_+^- \leq m^2 \leq v_+^+$ only. In order to illustrate the characteristics of the spectral weights $\varrho_\pm^{(t)}(m^2, m_t^2)$ we introduce their signature with

$$\Theta_\pm^{(t)}(m^2, m_t^2) = 2\frac{p_a(s)p_b(s)}{\pi}\varrho_\pm^{(t)}(m^2, m_t^2)|_{s=c_\pm^{(t)}(m^2)}, \quad (52)$$

which is an integer number depending on m^2 and m_t^2. For our first t-channel example both signatures are set to -1 and remain unchanged throughout the contours.

For our second t-channel process $\pi K \to \rho K^*$, there are six relevant critical points in the contour paths. The latter are indicated in Fig. 3 by their label number 1, 2, 7, 8, 9, 10. The positions of the circled numbers in the plot correspond to their numerical values as given in Table I. All such points are larger than the square of the exchange mass, in this case the pion mass, and therefore a proper evaluation of the spectral weight depends on those 6 critical points. The contour paths are off the real axis within the two intervals $v_-^- < m^2 < v_-^+$ and $v_+^- < m^2 < v_+^+$ only. In general, any of the critical points 7, 8, 9, 10 signals that the contour leaves or returns to the real axis. The corresponding critical contour points are surrounded by open circles in our plots. The anomalous point 2 characterizes the exchange mass $m^2 = t_-^+$ at which the $-$ contour hits a threshold or pseudothreshold pillar. Similarly, the condition $m^2 = t_+^+$ specifies the anomalous point 1 at which the $+$ contour hits a threshold or pseudothreshold pillar. In general either of the two contours may touch a threshold or pseudothreshold pillar only at any of the anomalous points 1, 2, 3, 4. If this occurs the contour runs towards the threshold along the real axis till it hits it and then inverts the direction and runs away from the threshold again. Whenever this happens the corresponding critical contour point is surrounded by an open square in our plots.

The associated spectral signatures are shown again left and right of the contour paths in the center of Fig. 3. Like for our first example we have $t_I^- \leq 0$ and $v_-^+ < v_+^-$ and the

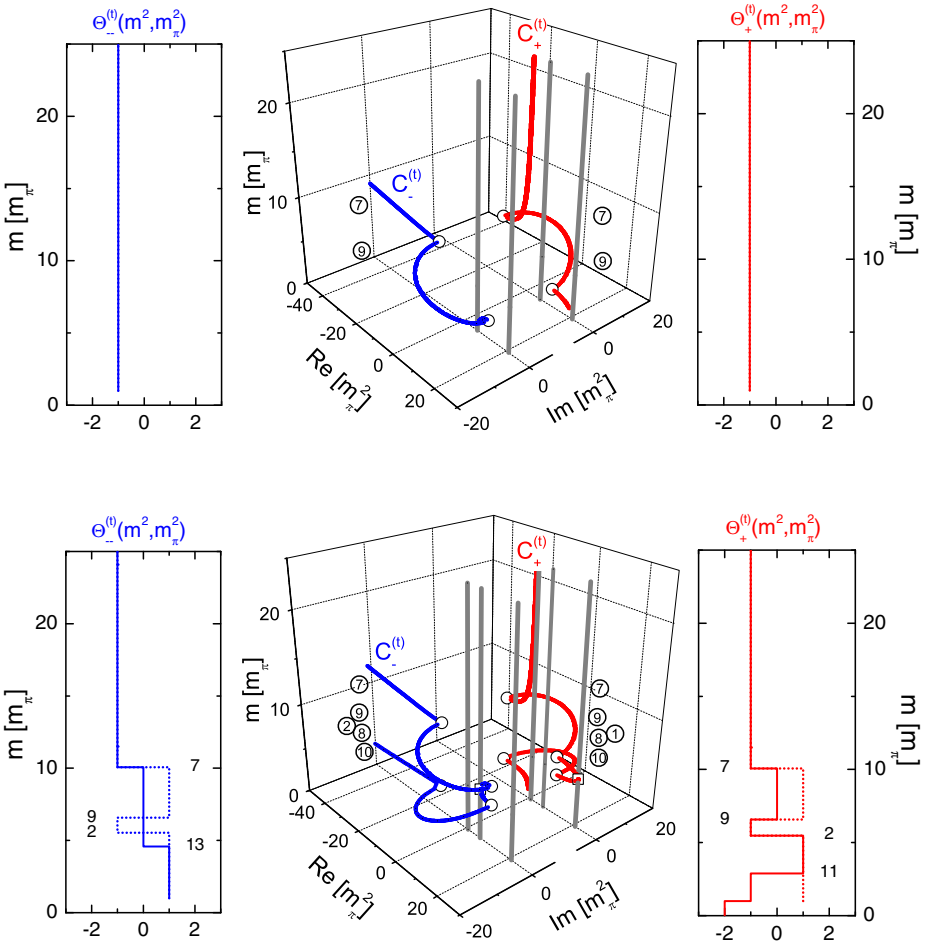

FIG. 3 (color online). Spectral signatures $\Theta_{\pm}^{(t)}(m^2, m_\pi^2)$ of (27) and (52) along the $c_{-}^{(t)}(m^2)$ (left column) and $c_{+}^{(t)}(m^2)$ (right column) contours for the t-channel processes $\pi K \to \pi K$ (upper panel) and $\pi K \to \rho K^*$ (lower panel) as functions of the mass of the exchanged particle m. The form of the two contours are shown in the center of the figure always. The thin pillars show the positions of relevant thresholds or pseudothresholds.

corresponding spectral weights are given by case 1 in (27) and (41). In contrast, however, the spectral signatures change several times now. In our plots the corresponding critical points are indicated by their label number as introduced in Table I. In particular, the extra terms (50) prove relevant here. This is so since $t_{-}^{+} > m_\pi^2$. We identify the associated closed contour. According to (43) the $-$ part is specified by $\bar{v}_{+}^{-} < m^2 < v_{+}^{+}$. The $+$ part receives two distinct contributions with $v_{+}^{-} < m^2 < v_{+}^{+}$ and $m^2 < \bar{v}_{+}^{+}$ [see (48)]. As a consequence of $t_{-}^{+} > t_{+}^{+}$ the additional critical points t_0 and $\bar{v}_{+}^{\pm}$ are activated in (50). Indeed at $m^2 = \bar{v}_{+}^{-}$ and $m^2 = \bar{v}_{+}^{+}$ the $-$ and $+$ spectral signatures are discontinuous, respectively. While in Fig. 3 the full lines show the full spectral signatures in the presence of the extra terms, the dotted lines show the results implied by (27) only. We do not show possible contributions for $m^2 < 0$ in the plots for the clarity of the presentation. Due to the condition $m^2 < \bar{v}_{+}^{+}$ discussed above they are present nevertheless in the $+$ spectral signature.

We turn to the remaining three t-channel processes that are illustrated in Fig. 4. The corresponding spectral signatures are shown left and right of the contour lines in the center of the plots. In all cases there are nontrivial changes of the signatures at the various critical points. The t-channel process $\pi\omega \to \rho\rho$ is characterized by the critical contour points 1, 4, 7, 8, 9 and the condition $t_I^{-} > 0$. With $v_{-}^{+} < v_{+}^{-} < v_{+}^{+}$ case 2 in (27) is implied. The conditions $m^2 = t_{+}^{+}$ and $m^2 = t_{-}^{-}$ identify at which point the $+$ and $-$ contours hit a threshold pillar, respectively. Moreover, the extra terms (44) are active since it holds $t_{-}^{-} > m_\pi^2$. The corresponding closed contour is identified in (43) and (46) which leads to $\bar{v}_{+}^{-} < m^2 < v_{+}^{+}$ and $v_{+}^{-} < m^2$ for the $-$ and $+$ parts, respectively.

With the t-channel process $\rho J/\Psi \to \pi\rho$ we have an example for case 3 in (27). The 6 critical contour points 1, 2, 7, 8, 9, 10 are active and we have $t_I^{-} \leq 0$ together with $v_{-}^{+} > v_{+}^{-}$. The extra terms in (50) are not probed here since we have $t_{+}^{+} < t_{-}^{+}$ together with $t_{-}^{-} < m_\pi^2$. Finally, the

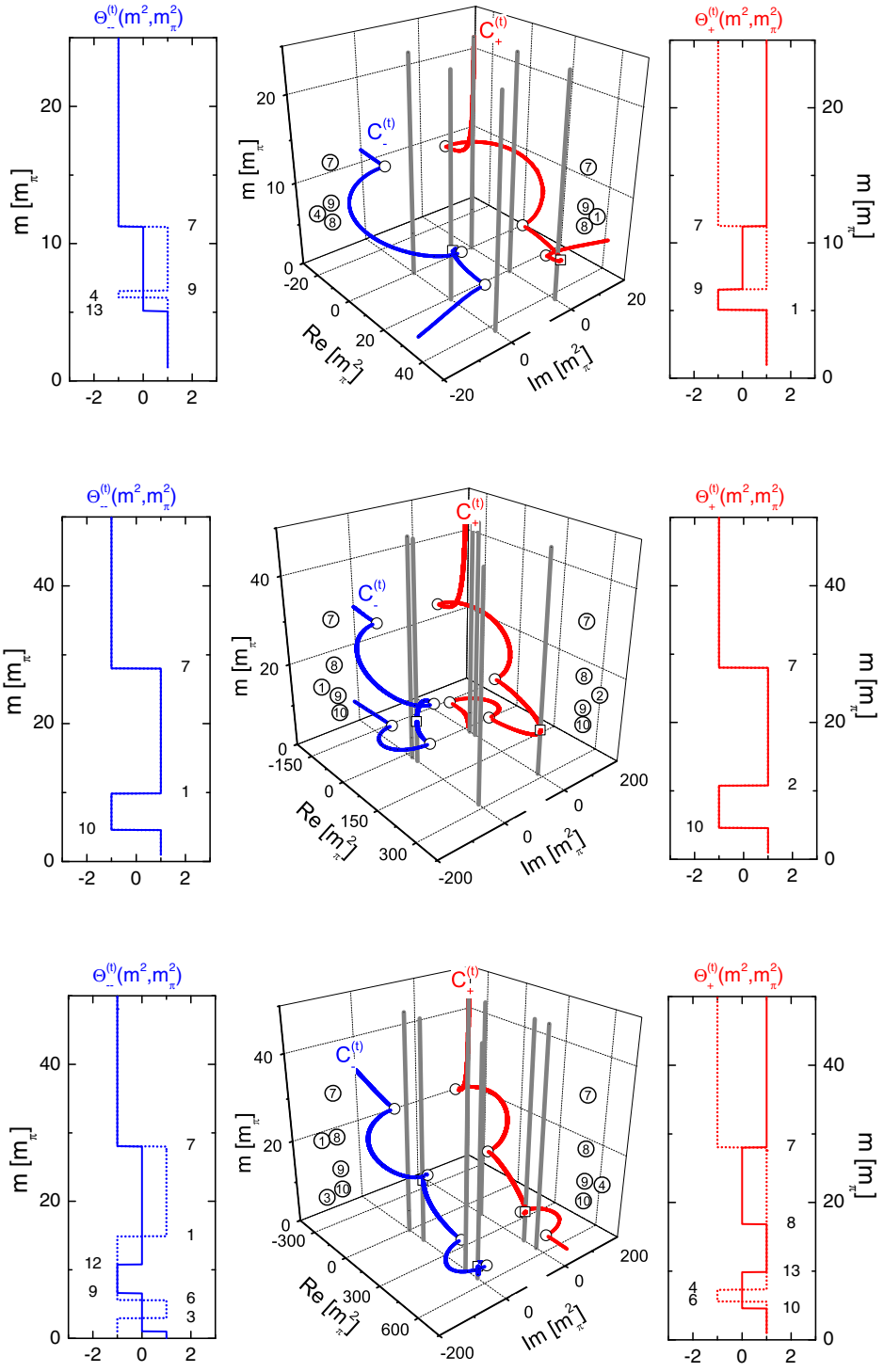

FIG. 4 (color online). Spectral signatures $\Theta_{\pm}^{(t)}(m^2, m_\pi^2)$ of (27) and (52) along the $c_{-}^{(t)}(m^2)$ (left column) and $c_{+}^{(t)}(m^2)$ (right column) contours for the t-channel processes $\pi\omega \to \rho\rho$, $\rho J/\Psi \to \pi\rho$ and $\pi J/\Psi \to \rho\rho$, respectively. The form of the two contours are shown in the center of the figure always. The thin pillars show the positions of relevant thresholds or pseudothresholds.

t-channel process $\pi J/\Psi \to \rho\rho$ illustrates case 4 in (27). The seven critical contour points 1, 3, 4, 7, 8, 9, 10 are active and we have $t_I^- > 0$ with $v_-^+ > v_+^-$. Since $t_+^+ > t_+^- > m_\pi^2$ the extra terms in (34) and in (44) are probed. While the first closed contour is specified with $\bar{v}_- < m^2 < v_+^-$ and $v_-^- < m^2 < \bar{v}_+^-$, the second closed contour is associated with the conditions $\bar{v}_-^+ < m^2 < v_+^+$ and $v_-^+ < m^2$ for the $-$ and $+$ parts, respectively.

We turn to the u-channel processes of Fig. 5. The list of critical exchange masses is collected in Table II, where

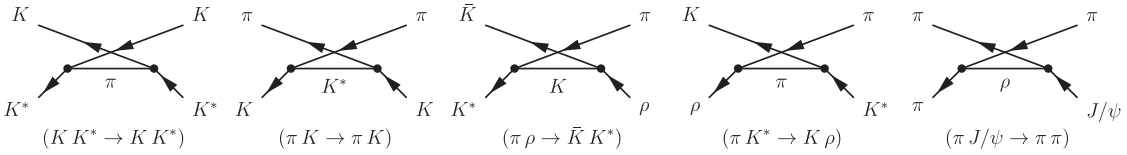

FIG. 5. Some specific u-channel exchange processes.

again the critical points are labeled through from 1 to 15. All dimension full quantities are expressed in units of the isospin averaged pion masses. We recall that a critical exchange mass is not necessarily active in the expression (27). Only if it is larger than the mass of the exchange particle it may turn relevant. The additional terms in the spectral density (41) as constructed in (34), (44), and (50) will be needed for our example cases. Our results are illustrated with Figs. 6 and 7 where besides the contour paths in the center of the plots, the signatures of the spectral weights as introduced with

$$\Theta_{\pm}^{(u)}(m^2, m_u^2) = 2\frac{p_a(s)p_b(s)}{\pi} Q_{\pm}^{(u)}(m^2, m_u^2)|_{s=c_{\pm}^{(u)}(m^2)} \tag{53}$$

are shown. There are integer numbers depending on m^2 and m_u^2. Like for our t-channel exchange studies the plots of the spectral signatures include solid lines that show the full signature with respect to (41) and dotted lines that correspond to the partial expressions (27). Possible contributions at $m^2 < 0$ are not shown for the clarity of the presentation. In all plots the relevance of a critical point is indicated by its label number as introduced in Table II.

Consider the first u-channel reaction $KK^* \to KK^*$ of Fig. 5 and Fig. 6. With $u_I^- > 0$ and $v_-^+ < v_+^-$, case 2 in (27) is selected. This is our first case with $u_+^- > 0$. As a consequence both contour lines pass through the threshold and pseudothreshold of this reaction, i.e. $(m_K \pm m_{K^*})^2$. This occurs at the critical points $m^2 = u_+^+ = u_+^- > m_\pi^2$ and $m^2 = u_-^+ = u_-^- > m_\pi^2$. Since in this reaction a π meson is exchanged the relevant parts of the contours do reach both threshold points. After all it holds $u_+^- > m_\pi^2$. Therefore it appears that the extra terms (34), properly transformed from the t-channel kinematics to the u-channel kinematics with $t \leftrightarrow u$, are active in this case. The associated closed contour is characterized by $\bar{v}_-^- < m^2 < v_-^+$ and $v_-^- < m^2 < \bar{v}_-^+$. However, since $\bar{v}_-^- = v_-^+$ and $v_-^- = \bar{v}_-^+$ these are empty conditions for the given example and none of the terms in (34) are relevant. On the other hand we may find a contribution of (44) since $u_-^- > m_\pi^2$. Here the conditions for the closed contour are $\bar{v}_+^- < m^2 < v_+^+$ and $v_+^- < m^2 < \mathrm{Max}(\bar{v}_+^+, v_+^+)$. Since $\bar{v}_-^+ = v_-^-$ and $\bar{v}_-^- = \mathrm{Min}(v_-^+, v_+^-)$ again these are empty conditions. Correspondingly, there is no effect of the extra terms (44) also.

Inspecting the contour paths in Fig. 6 one may be led to the conclusion that the corresponding partial-wave projected amplitude has a branch cut going through the two threshold points. However, this is not so. The effect of the $+$ and $-$ contours in (6) cancel in part, so that the full contribution does not have such a branch cut. Nevertheless, a branch cut emerges on the real axis, however, only at energies where the $+$ and $-$ contours do not overlap.

TABLE II. Critical points for the u-channel exchange processes shown in Fig. 5, in units m_π^2.

		$KK^* \to KK^*$	$\pi K \to \pi K$	$\pi\rho \to \bar{K}K^*$	$\pi K^* \to K\rho$	$\pi J/\psi \to \pi\pi$
1	u_+^+	8.32172	6.71244	31.9405	22.2027	251.181
2	u_-^+	101.333	21.0758	91.8556	135.925	∞
3	u_+^-	8.32172	6.71244	−2.87974	5.87230	−21.4357
4	u_-^-	101.333	21.0758	53.8542	40.9191	23.4357
5	u_I^+	54.8272	13.8941	44.4880	70.8985	∞
6	u_I^-	54.8272	13.8941	42.8973	31.5609	1
7	v_+^+	101.333	21.0758	84.0703	101.333	549.234
8	v_-^+	8.32172	6.71244	29.9819	20.9594	459.491
9	v_+^-	101.333	21.0758	55.8842	43.2720	4
10	v_-^-	8.32172	6.71244	3.94940	8.32172	0
11	$\bar{v}_+^+$	101.333	21.0758	145.925	−270.515	−21.4357
12	$\bar{v}_-^+$	8.32172	6.71244	37.4141	25.9791	23.4357
13	$\bar{v}_+^-$	101.333	21.0758	48.2445	35.0822	251.181
14	$\bar{v}_-^-$	8.32172	6.71244	−46.4972	−5.11443	∞
15	u_0	109.654	27.7882	87.3853	102.459	∞

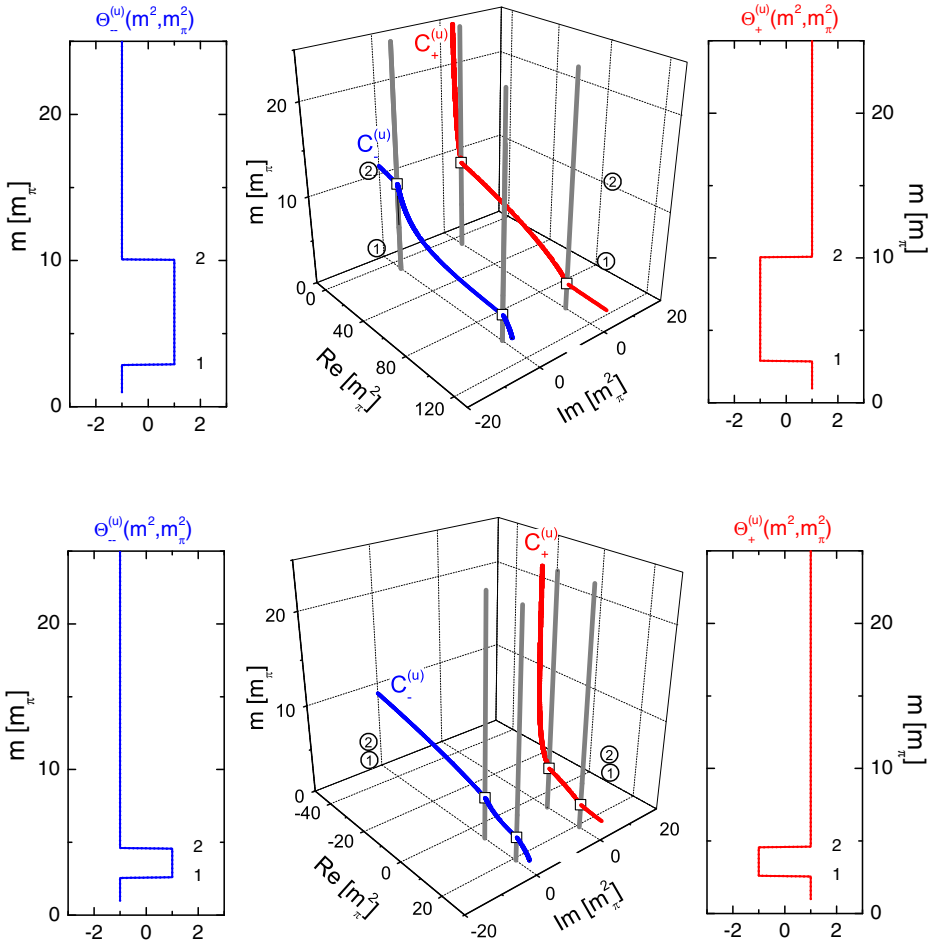

FIG. 6 (color online). Spectral signatures $\Theta_{\pm}^{(u)}(m^2, m_\pi^2)$ along the $c_{-}^{(u)}(m^2)$ (left column) and $c_{+}^{(u)}(m^2)$ (right column) contours for the u-channel processes $KK^* \to KK^*$ and $\pi K \to \pi K$ as functions of the mass of the exchanged particle m. The form of the two contours are shown in the center of the figure always. The thin pillars show the positions of relevant thresholds or pseudothresholds.

This follows since the $+$ and $-$ spectral signatures have opposite sign. As a consequence there is a branch cut connecting the two particular points $c_{+}^{(u)}(m_\pi^2) > (m_K + m_{K^*})^2$ and $c_{-}^{(u)}(m_\pi^2) > (m_K + m_{K^*})^2$. Here we have an example where a left-hand branch cut is located right to the largest threshold pillar.

We discuss the $\pi K \to \pi K$ process of Fig. 6. This is a further example with $u_{+}^{-} > 0$ where case 2 in (27) is scrutinized. Again both contour lines pass through the threshold and pseudothreshold of this reaction, i.e. $(m_\pi \pm m_K)^2$. This occurs at the critical points $m^2 = u_{+}^{+} = u_{+}^{-}$ and $m^2 = u_{-}^{+} = u_{-}^{-}$. Since in this reaction a K^* meson is exchanged, with a mass distribution starting at $(m_\pi + m_K)^2 > u_{-}^{-} > u_{+}^{-}$, the relevant parts of the contours do not reach any of the threshold points, however. Like in our first example, even though we have $u_{-}^{-} > m_\pi^2$ and $u_{+}^{-} > 0$, there are no contributions from (34) and (44). This is so independent on the value of the exchange mass m_u. In Fig. 6 the contour lines are shown for $m > m_\pi$, in order to illustrate the generic mechanism.

There are the remaining u-channel exchange processes analyzed in Fig. 7. The first two reactions $\pi\rho \to \bar{K}K^*$ and $\pi K^* \to K\rho$ probe the case 2 in (27) with $v_{-}^{+} < v_{+}^{-}$. The extra terms in (34) prove relevant for the second reaction with $u_{+}^{-} > m_\pi^2$ only. The corresponding closed contour path is generated by the condition $\bar{v}_{-}^{-} < m^2 < v_{-}^{+}$ and $v_{-}^{-} < m^2 < \bar{v}_{-}^{+}$ for the minus and plus contours, respectively, [see (33)]. In contrast, the additional terms (44) are needed in both cases. For the reaction $\pi\rho \to \bar{K}K^*$ it holds $u_{-}^{-} > m_K^2$ and the closed contour is given by $\bar{v}_{+}^{-} < m^2 < v_{+}^{+}$ and $v_{+}^{-} < m^2 < \bar{v}_{+}^{+}$. A slightly different condition is derived for the $\pi K^* \to K\rho$ reaction with $u_{-}^{-} > m_\pi^2$. Here the closed contour follows from $\bar{v}_{+}^{-} < m^2 < v_{+}^{+}$ and $v_{+}^{-} < m^2$ instead.

We discuss the final u-channel reaction $\pi J/\psi \to \pi\pi$. It is described by the case 4 in (27) with $v_{-}^{+} > v_{+}^{-}$. Since it holds $u_{+}^{-} < 0$ here the extra terms (34) are not active. On the other hand with $u_{+}^{+} > m_\rho^2$ the terms (44) are needed. The corresponding closed contour follows with $\bar{v}_{-}^{+} < m^2 < v_{+}^{+}$ and $v_{-}^{+} < m^2$.

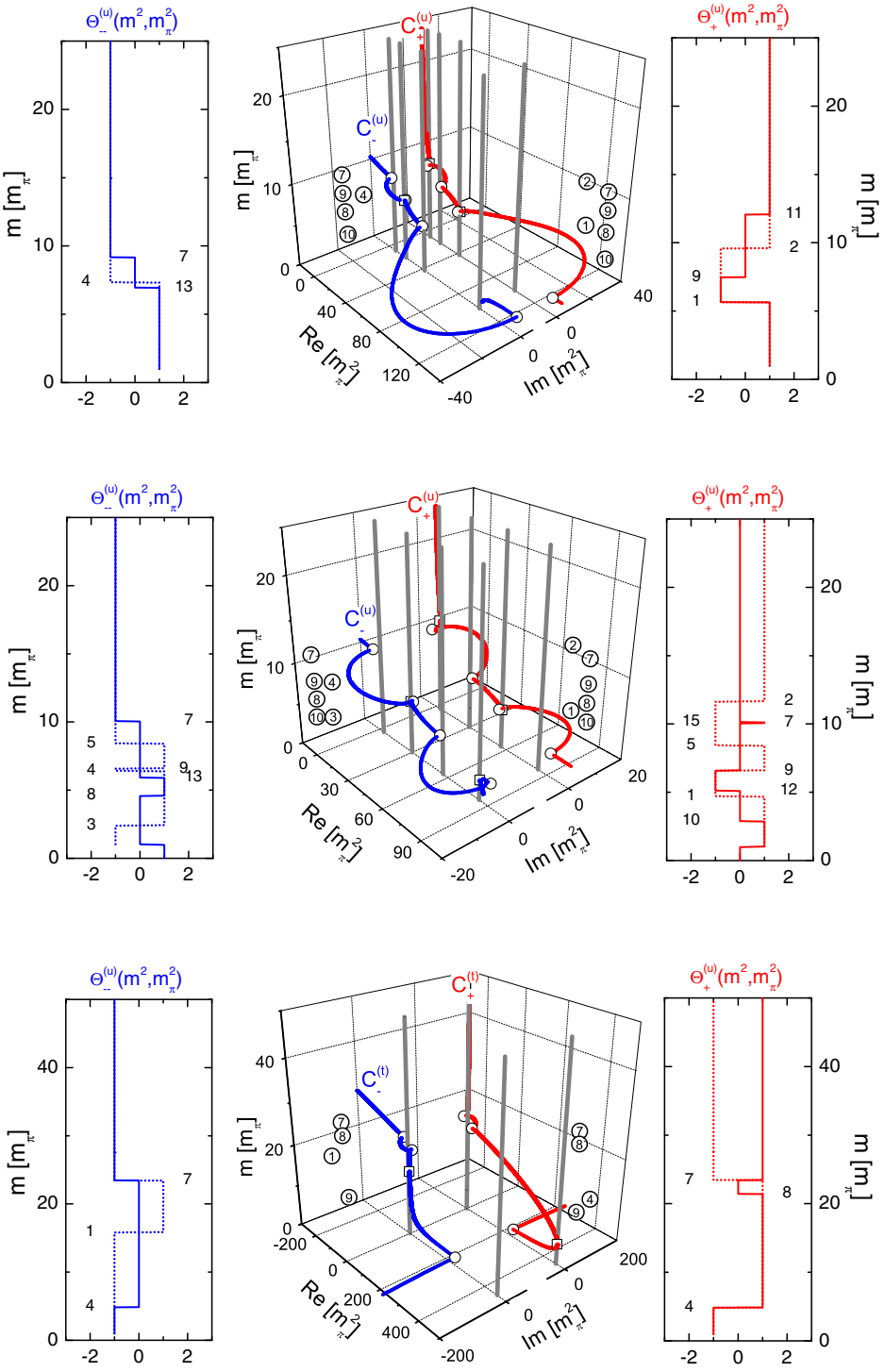

FIG. 7 (color online). Spectral signatures $\Theta_{\pm}^{(u)}(m^2, m_\pi^2)$ along the $c_{-}^{(u)}(m^2)$ (left column) and $c_{+}^{(u)}(m^2)$ (right column) contours for the u-channel processes $\pi\rho \to \bar{K}K^*, \pi K^* \to K\rho$ and $\pi J/\Psi \to \pi\pi$. The form of the two contours are shown in the center of the figure always. The thin pillars show the positions of relevant thresholds or pseudothresholds.

A concluding remark on the numerical implementation of (6) is in order here. A partial cancellation of the + and − contour contributions in (6) occurs frequently. Whenever the two contours run along identical regions on the real axis this may happen. In a numerical implementation of (6) it is useful to work out such cancellations explicitly. Based on our general results, this is straightforwardly achieved in a computer code.

V. SUMMARY

We have analyzed the generic structure of partial-wave projected t- and u-channel exchange diagrams. A general and explicit form for a dispersion-integral representation for their contributions to partial-wave reaction amplitudes was established. Our results hold for the case of overlapping left- and right-hand cut structures, decaying particles and anomalous thresholds or pseudothresholds. Various applications to specific examples were worked out and illustrated in detail.

With our study, more realistic treatments of final state interactions in the resonance region of QCD may become feasible. The merit of the result lies in its generality. It is a convenient basis for coupled-channel theories with a large number of channels involved, where a case-by-case study is prohibitive.

ACKNOWLEDGMENTS

M. F. M. Lutz thanks J. Hofmann for collaboration at an early stage of the project. C. L. Korpa was partially supported by Országos Tudományos Kutatási Alapprogramok (OTKA, Hungary) Grant K109462.

[1] F. Zachariasen and C. Zemach, Phys. Rev. **128**, 849 (1962).
[2] R. Dalitz, T. Wong, and G. Rajasekaran, Phys. Rev. **153**, 1617 (1967).
[3] R. Logan and H. Wyld, Phys. Rev. **158**, 1467 (1967).
[4] N. Kaiser, P. Siegel, and W. Weise, Nucl. Phys. **A594**, 325 (1995).
[5] A. Gómez Nicola and J. R. Pélaez, Phys. Rev. D **65**, 054009 (2002).
[6] M. F. M. Lutz and E. E. Kolomeitsev, Nucl. Phys. **A700**, 193 (2002).
[7] M. F. M. Lutz, G. Wolf, and B. Friman, Nucl. Phys. **A706**, 431 (2002).
[8] E. E. Kolomeitsev and M. F. M. Lutz, Phys. Lett. B **585**, 243 (2004).
[9] M. F. M. Lutz and E. E. Kolomeitsev, Nucl. Phys. **A730**, 392 (2004).
[10] A. M. Gasparyan and M. F. M. Lutz, Nucl. Phys. **A848**, 126 (2010).
[11] I. Danilkin, A. M. Gasparyan, and M. F. M. Lutz, Phys. Lett. B **697**, 147 (2011).
[12] I. Danilkin, L. Gil, and M. F. M. Lutz, Phys. Lett. B **703**, 504 (2011).
[13] A. Gasparyan, M. F. M. Lutz, and E. Epelbaum, Eur. Phys. J. A **49**, 115 (2013).
[14] I. Danilkin, M. F. M. Lutz, S. Leupold, and C. Terschlüsen, Eur. Phys. J. C **73**, 2358 (2013).
[15] G. Chew and F. Low, Phys. Rev. **101**, 1570 (1956).
[16] S. Mandelstam, Phys. Rev. **112**, 1344 (1958).
[17] G. Chew and S. C. Frautschi, Phys. Rev. Lett. **7**, 394 (1961).
[18] G. Frye and R. L. Warnock, Phys. Rev. **130**, 478 (1963).
[19] J. Ball, R. Garg, and G. L. Shaw, Phys. Rev. **177**, 2258 (1969).
[20] C. K. Chen, Phys. Rev. D **5**, 1464 (1972).
[21] R. J. Eden, P. V. Landshoff, D. I. Olive, and J. C. Polkinghorne, *The Analytic S-Matrix* (Cambridge University Press, Cambridge, England, 1966).
[22] P. W. Johnson and R. L. Warnock, J. Math. Phys. (N.Y.) **22**, 385 (1981).
[23] A. Gasparyan, M. F. M. Lutz, and B. Pasquini, Nucl. Phys. **A866**, 79 (2011).
[24] J. Kennedy and T. D. Spearman, Phys. Rev. **126**, 1596 (1962).
[25] J. Petersen, Nucl. Phys. **B13**, 73 (1969).
[26] L. Kok, J. Greben, and F. van der Ploeg, Ann. Phys. (N.Y.) **79**, 386 (1973).
[27] M. F. M. Lutz and E. E. Kolomeitsev, Found. Phys. **31**, 1671 (2001).
[28] M. F. M. Lutz and E. E. Kolomeitsev, Nucl. Phys. **A730**, 110 (2004).
[29] E. E. Kolomeitsev and M. F. M. Lutz, Phys. Lett. B **582**, 39 (2004).
[30] M. F. M. Lutz and M. Soyeur, Nucl. Phys. **A813**, 14 (2008).
[31] J. Hofmann and M. F. M. Lutz, Nucl. Phys. **A763**, 90 (2005).
[32] J. Hofmann and M. F. M. Lutz, Nucl. Phys. **A776**, 17 (2006).
[33] C. Terschlüsen, S. Leupold, and M. F. M. Lutz, Eur. Phys. J. A **48**, 190 (2012).
[34] T. Trueman, Phys. Rev. **173**, 1684 (1968).
[35] M. King and P. Kuo, Phys. Rev. D **1**, 442 (1970).
[36] G. Tindle, Phys. Rev. D **11**, 1688 (1975).
[37] W. A. Bardeen and W. Tung, Phys. Rev. **173**, 1423 (1968).
[38] F. Cheung and F. S. Chen-Cheung, Phys. Rev. D **5**, 970 (1972).
[39] S. Stoica, M. F. M. Lutz, and O. Scholten, Phys. Rev. D **84**, 125001 (2011).
[40] M. F. M. Lutz and I. Vidana, Eur. Phys. J. A **48**, 124 (2012).
[41] Y. Heo and M. F. M. Lutz, Eur. Phys. J. A **50**, 130 (2014).
[42] T. Kibble, Phys. Rev. **117**, 1159 (1960).
[43] W. R. Frazer and J. R. Fulco, Phys. Rev. **119**, 1420 (1960).
[44] R. Karplus, C. M. Sommerfield, and E. H. Wichmann, Phys. Rev. **111**, 1187 (1958).
[45] S. Mandelstam, Phys. Rev. Lett. **4**, 84 (1960).
[46] M. Stingl and A. S. Rinat, Phys. Rev. C **10**, 1253 (1974).
[47] A. S. Rinat and M. Stingl, Ann. Phys. (N.Y.) **65**, 141 (1971).